DETERMINATION OF CROSS SECTIONS FOR ION-ATOM INTERCHANGE REACTIONS

By
MANUEL G. MENENDEZ

A DISSERTATION PRESENTED TO THE GRADUATE COUNCIL OF
THE UNIVERSITY OF FLORIDA
IN PARTIAL FULFILLMENT OF THE REQUIREMENTS FOR THE
DEGREE OF DOCTOR OF PHILOSOPHY

UNIVERSITY OF FLORIDA
April, 1963

ACKNOWLEDGMENT

The author would like to thank Drs. T. L. Bailey and E. E. Muschlitz, Jr., co-chairmen of his supervisory committee, for their continued interest and guidance in the carrying out of this research. He also wishes to thank the other members of his supervisory committee for their helpful suggestions in the writing of this dissertation. He further wishes to thank his colleague Mr. D. W. Vance for his assistance in obtaining the data.

The author is indebted to the U. S. Office of Naval Research and the National Science Foundation for their financial support of this research.

This dissertation is dedicated to Sandra.

TABLE OF CONTENTS

LIST OF FIGURES

CHAPTER I

INTRODUCTION

Since many chemical reactions and physical changes involve collisions of atomic species, or at least their interaction at close range, studies of atomic and molecular collisions are of great importance to the understanding of a broad range of natural phenomena. One of the most effective experimental methods of studying collisional phenomena is by beam-gas scattering techniques. In such experiments an atomic, ionic, or molecular beam with a well-defined energy is directed through a gas of target atoms or molecules at a known density. The effects of the collisions between beam and target particles are then deduced from measurements of the currents of product species.

Collisions are normally classified into two categories, namely: (a) elastic collisions--in which there is no change in the internal energy state of the colliding particles, and (b) inelastic collisions--in which the internal energy state of at least one of the colliding species is altered.

For a given colliding system, the differential and total elastic scattering cross sections are determined by the relative velocity of the colliding particles and their force of interaction. For realistic interaction potentials, it can be shown (1,2) that

elastic scattering usually results in quite small deflections of the colliding particles. For beam-gas scattering experiments, in which energetic primary beam particles are scattered by target atoms or molecules with very small initial kinetic energies it follows that the primary beam particles which undergo elastic scattering are strongly collimated in the primary beam direction, and have nearly the same velocities as the primary beam particles. The dependence of the observed elastic scattering cross-sections upon relative velocity of collision has been used to calculate empirical interaction potential laws (2). This type of analysis has been applied to a variety of systems, for example, fast neutral atom-neutral atom interactions (3) positive ion-atom interactions (4), and negative ion-atom interactions (5).

Inelastic collisions may involve a transfer of internal energy, a transfer of one or more electrons, or the formation of new molecular species. In contrast to the case of elastic scattering, it is no longer usually true that most of the initial momentum and kinetic energy of the colliding system resides in one of the reaction products. Instead, the collision kinetic energy can be shared in a variety of ways, and, in many cases the product species can be scattered through large angles.

This work is primarily concerned with the measurement of cross-sections for inelastic processes occurring in positive ion-molecule systems over the energy range from 10 ev to 130 ev. The processes which were important in this energy range were of the types:

(i) $A^+ + B = B^+ + A$: charge transfer

(ii) $X_2^+ + A = X^+ + X + A$: collision-induced dissociation

(iii) $X_2^+ + Y = XY^+ + X$: ion-molecule reaction.

Special emphasis was placed on reactions of type (iii). These are perhaps the simplest chemical reactions which can be studied by direct physical means. Previous studies of these reactions have indicated that the cross-sections may be from a small fraction to several times larger than gas kinetic.

There are a large number of positive ion-molecule systems of interest for which there exists a maximum angle of scattering for the molecular ion produced via an ion-molecule reaction. It was with this particular case in mind that the two experiments to be described were designed.

The two systems studied were H_2^+ in Ar and H_2^+ in H_2. The method used for this study was to direct a well-defined mass-analyzed ion beam from a magnetic mass spectrometer through a field-free region, the reaction region, filled with scattering gas at a known pressure and temperature. The product ions formed by collisions in the reaction region were analyzed by two methods.

In the first method which will be called the DC retardation experiment, the energy of the ions was measured and this was used to distinguish different groups of product ions. The measured energies of product ions will be referred to as the "energetics" of the system in the remainder of the text. Figure 1 shows the collision chamber used in this experiment. The product ions formed in the reaction region, defined by the electrodes D, B, F, and A, are retarded and turned back by applying a positive

potential, V_R, to the DC retarding grid (electrode R). Ions possessing different energies are turned back by different values of V_R. They are ultimately collected on electrodes F and B which are connected to an electrometer. This experiment is capable of accurately measuring the total inelastic cross-section along with determining the energetics of the inelastic processes. It will be seen that for some but not all collision systems, a knowledge of the energetics, i.e., the energy of the product ions, leads to positive identification of the products.

The second method, which will be called the RF experiment, employs a radio-frequency mass spectrometer for mass analysis of the product ions. The radio-frequency mass spectrometer is installed beyond the same reaction region electrode structure used in the DC retardation experiment. This arrangement, shown in Figure 2, is capable of identifying the products formed and of determining the relative currents of such product ions. These two types of experiments complement each other; studies of a given system using both experimental methods can in many cases give accurate cross-sections for each of the various inelastic processes which take place.

These two new experimental methods, to be described in detail in the following chapters, are particularly useful for the study of ion-molecule reactions. A large amount of experimental information concerning ion-molecule reactions has been obtained by studies carried out in more or less conventional mass spectrometer electron impact ion sources (6). In particular, Field, Franklin, and Lampe (7) and Stevenson and Schissler (8)

have applied an ingenious analysis to the results of their ion-source experiments in which an electron beam produces primary ions which in turn react with neutral particles as they are accelerated out of the ion source. They have found many ion-molecule reactions to have high, temperature-independent specific rate constants. However, an ion-source type of experiment is not without its difficulties; the energy of the primary ions is not well known, the path length is not well-defined, the reactions occur in the presence of electric and magnetic fields, and sometimes the reactant ions are not known with certainty. Recently, Giese and Maier (9) have studied ion-molecule reactions in a double magnetic-type mass spectrometer experiment. One mass spectrometer is used to define the incident ion beam and the other magnetic mass spectrometer is used to mass analyze the products. This experimental arrangement is capable of determining the energy dependence of the ion-molecule reaction cross-sections. However, it is necessary in this experiment, to refocus the products from the reaction region into the magnet chamber of the product mass analyzer. It will be seen that many of the difficulties mentioned above for the ion-source type of experiment are obviated by the design of the present experimental arrangement.

The H_2^+, Ar system was studied in the DC retardation experiment and cross-sections for charge transfer, ion-molecule reaction producing ArH^+, and collision-induced dissociation were obtained over the energy range from 10 to 130 ev. The

H_2^+, H_2 system was studied in the DC retardation experiment yielding cross-sections for charge transfer and total reaction. This system was also studied in the RF experiment and H_2^+ due to charge transfer and H_3^+ due to ion-molecule reaction were identified. It was impractical to continue the investigation in order to obtain a relative cross-section for the different processes due to insufficient incident ion current. However, enough data were taken to support the concept of the experiment.

CHAPTER II

EXPERIMENTAL METHODS

General Design Considerations

If the conservation of energy and momentum is applied to the following system,

$$A^+ + B = C^+ + D \pm \Delta E \quad , \qquad [1]$$

which is typical of an ion-molecule reaction, it can be shown (10) that a maximum angle of scattering of the observed product C^+ exists for systems for which the parameter

$$\gamma = + \left[\frac{M_A M_C}{M_B M_D} \frac{E}{E+\Delta E} \right]^{1/2} \geq 1 \quad , \qquad [2]$$

where E is the energy associated with the relative motion and ΔE is the energy defect of the reaction. This maximum angle in the laboratory system of coordinates is given by

$$\theta_{max} = \sin^{-1} \frac{1}{\gamma} \quad . \qquad [3]$$

There are many positive ion-molecule systems of interest for which the maximum angle of scattering is less than 45°. It was with this in mind that an open collision chamber, shown in Figure 1, to include reaction region, subsequent plane grids, and collector, was designed. The largest angle through which

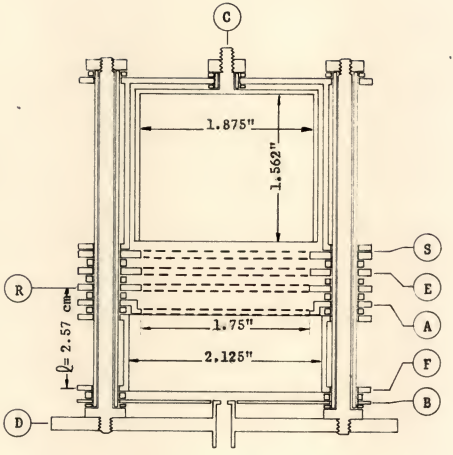

Figure 1.—DC Retardation Experiment Collision Chamber

particles can be scattered and still emerge from the reaction region is 46.5°. This limiting angle is defined as the angle between a line drawn through the 2 mm hole in the final defining electrode, D, and a line from the center of the 2 mm hole to the inner radius of the top grid of the reaction region, electrode A.

It is possible, then, to extract or retard ions of different energies formed in the reaction region by adjusting the potentials on the appropriate grids above the reaction region. In this way it is possible to measure all currents due to ions formed from inelastic processes that are scattered in the forward direction, provided that the deviation of these ions does not exceed the limiting angle (46.5°) and to measure the energetics of these ions as well as to mass analyze them. Any ions that are not scattered in the forward direction will be collected on the reaction region walls, electrodes B and F. The energy of these ions can be inferred from the behavior of this current upon extraction.

Figure 2 shows the experimental arrangement used in the RF experiment. The RF mass analysis region is composed of plane open grids in accord with the general considerations mentioned above. The mass analysis of the product ions is accomplished by a linear radio-frequency mass spectrometer. It is pertinent at this point to briefly discuss the operation of a linear radio-frequency mass spectrometer originally designed by W. H. Bennett (11). The operation of the radio-frequency mass spectrometer is discussed in terms of small signal operation (12).

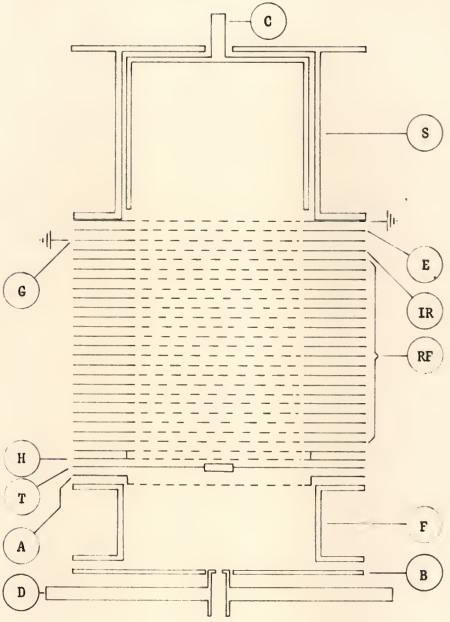

Figure 2.—Schematic of RF Experiment Collision Chamber

The instrument consists of 20 plane-parallel, equidistant, RF grids and a DC retarding grid. Alternate grids of the RF electrode system are grounded and the other grids have applied to them a sinusoidal RF voltage. The operation of the RF system is based on velocity selection. Ions to be mass analyzed are accelerated through a DC voltage into the radio-frequency electrode system. Some ions gain more energy through the RF system than others as follows.

If the time of transit of an ion between two RF grids is half the radio-frequency period, then this ion will remain in synchronism with the applied RF field. When the synchronous ion enters the RF electrode system at a particular time with respect to the applied RF field, this ion will gain more energy than any other. As the ions leave the RF electrode system they encounter a DC retarding potential barrier (called the RF retarding potential barrier, in order to avoid confusion with the DC retardation grid) which rejects all but the most energetic ions. Thus only the ions that stay in synchronism with the RF field are able to reach the collector. The mass (amu) to charge number ratio of this ion is given by

$$\frac{m}{n} = K \frac{V_o}{f^2 d^2} \quad , \qquad [4]$$

where $K = 0.0746$, V_o is the accelerating voltage, n is the charge number of the ion, d is the distance between adjacent RF grids in inches and f is the frequency in mc/s.

In general, the energy gained, ΔW, is a function of the parameter α, the transit angle, where

$$\alpha = 2\pi fd \left[\frac{m}{2eV_o}\right]^{1/2} .$$

For the synchronous ion $\alpha = \pi$. The maximum energy gained for the synchronous ion is given by (12)

$$\Delta W = \frac{2NnV}{\pi} \text{ for } \alpha = \pi \quad , \qquad [5]$$

where N is the number of stages, n is the charge number of the ion, and V is the rms RF voltage. The resolution of the instrument and collection efficiency of the synchronous ion are related by the following expression (12), $RE = N/8\sqrt{3}$, where, R is the resolution and E is the collection efficiency. It can be seen that for a given number of stages, N, the product of resolution and collection efficiency is a constant. The above relationships hold for small signal operation, i.e., when the energy gained through the RF system is small when compared to the DC accelerating voltage. The RF spectrometer used in this work was not always operated under small signal conditions; hence it was necessary to determine the maximum energy gained experimentally for each ion being mass analyzed. For a more detailed analysis of the RF mass spectrometer the original papers should be consulted (11,12). The plane open RF grids allow the RF mass spectrometer to analyze broad beams. This arrangement of open reaction region and open mass analysis region, shown schematically in Figure 2, is capable of mass analyzing

broad beams and does not require the refocusing of product ions into a narrow beam which would be necessary for magnetic mass analysis of the product ions.

One of the salient features of the operation of the RF mass spectrometer in the current application was the need for a target (electrode T in Figure 2). The purpose of electrode T is twofold: it intercepts the primary unscattered beam and prevents primary ions from entering the RF mass analysis region and it acts as a collector for the primary ion beam. Electrode T is essential for the mass analysis of product ions as will be shown in the following discussion. First, without the target, electrode T, one is limited to the study of reactions in an energy range not to exceed the maximum energy gained through the RF system given by equation [5]. If the primary ion energy, W_p, is greater than the maximum energy gained through the RF system $(\Delta W)_{max}$, then it would take an RF ion-retarder potential barrier, V_{IR}, equal to W_p(i.e., $V_{IR}=W_p$) to stop the primary beam and hence effect mass analysis of the product ions. But since the product ion can only gain an energy equal to $(\Delta W)_{max}$ through the RF system and since it was stipulated that $W_p > (\Delta W)_{max}$, they will not have sufficient energy to overcome V_{IR}; hence the product ion will not reach the collector. This case is shown on a DC potential diagram, Figure 3. It is shown for the case where the frequency corresponds to the resonant frequency of the product ion and further it is assumed that the primary beam ions are not gaining any energy

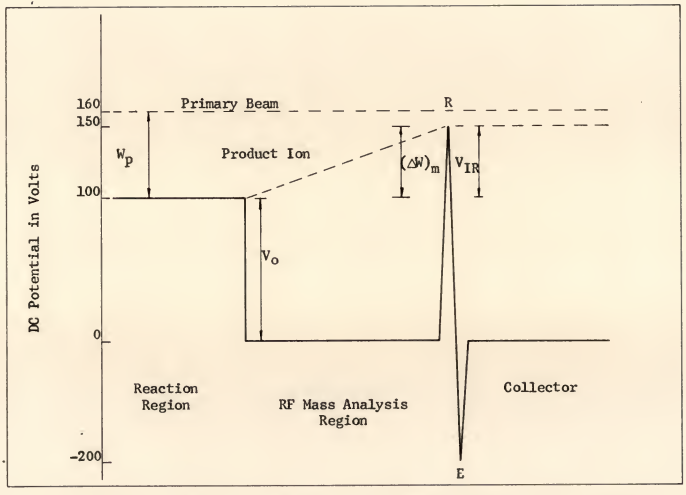

Figure 3.--DC Potential Profile for the RF Experiment without Target

through the RF system. This limitation in the incident ion energy, W_p, which in practice was from 10 ev to 30 ev since $(\Delta W)_{max}$ was about 50 ev was undesirable.

Second, assuming one wishes to stay within the energy range predicated by the above condition another difficulty associated with the resolution of the instrument arises. It is that in order to detect a product ion V_{IR} must be lower than $(\Delta W)_{max}$, the maximum energy gained by the product ion. However, the energy gained by the primary beam at the resonant frequency of the product ion is not zero but some value $\Delta W(\alpha \neq \pi)$. Hence, the primary beam has an energy $[W_p + \Delta W(\alpha \neq \pi)]$ emerging from the RF region. The result is that a given RF ion-retarder potential barrier, V_{IR}, corresponding to a high resolution for the secondaries corresponds to a low resolution for the primaries. Since the current due to primary ions is usually of the order of 100 times as large as that due to a product ion and the resolution for the primary beam particles is low, peaks due to primary ions appear at frequencies other than the resonant frequencies of the primary beam. That is $\Delta W(\alpha \neq \pi)$, the energy gained by the primary beam at frequencies other than the primary beam resonant frequency, is large enough that when this energy is added to the incident ion energy, W_p, the primary beam is able to overcome V_{IR} and reach the collector. These "satellite" peaks arising from primary ions which gain appreciable energy from the RF field at non-resonant frequencies, were for the most part intense enough to obscure the frequency range in which product ions were expected to appear.

Hence, it was determined that mass analyzed product ions would only be detected if the primary beam could be stopped or collected somewhere after the reaction region and before the RF region. The introduction of the target accomplished this purpose and also provided a way for monitoring the primary beam to insure steady conditions.

The final arrangement as shown in Figure 2 is not without its limitation, since the target intercepts an appreciable fraction of the product ion current. The low product ion mass analyzed current was a limitation in the RF experiment. The primary ion current was approximately 100 times less than is normal for this type of ion source. Some modifications were attempted in order to improve the initial ion current, however, it was concluded that the entire apparatus needed to be cleaned and realigned.

Apparatus

A schematic of the over all apparatus is shown in Figure 4. The apparatus, except for the collision chambers, secondary analyzer region, and detection systems, is the same as that described by Cramer and Simons (13). The ions are formed in a high pressure electron bombardment source, focused into the magnetic field region for mass separation, refocused into an energy defining region maintained at the same potential as the reaction region, and finally collimated by the final defining electrode, D, into the reaction region. The entire apparatus is

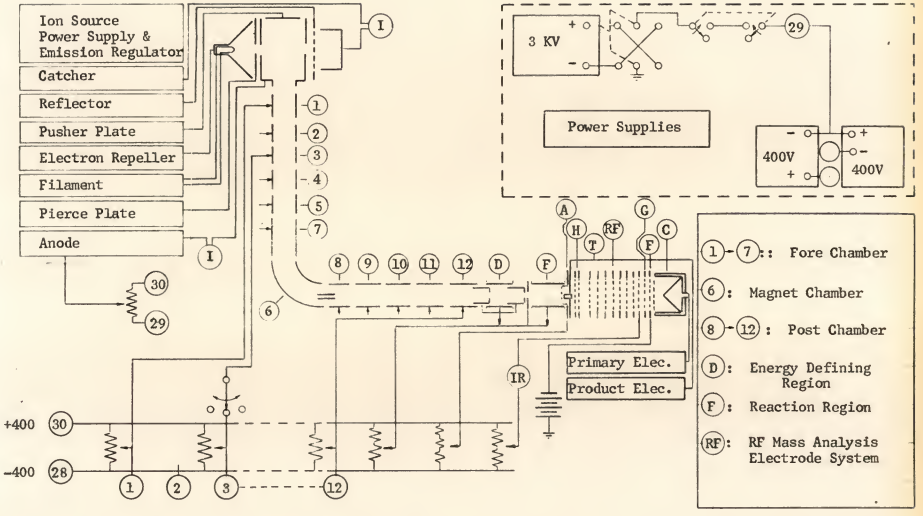

Figure 4.—Apparatus (Schematic)

cylindrically symmetrical about the ion beam axis. The reaction region, RF grid support rings, DC grid support rings, and the focusing elements are made of free machining brass that has been gold-plated. Figure 1 shows construction details which are applicable to both experimental arrangements.

The DC grids are made of a tungsten mesh of approximately 92 per cent transmission. The tungsten mesh lies between the gold-plated DC grid support ring and a thin nickel annular ring in sandwich form held in place by spot welds between the gold-plated support rung and the nickel annular ring.

The RF grid support rings were strung with nickel wire 0.002" in diameter through holes in the RF grid support rings. The holes were spaced such that the nickel wire formed open squares 1/8" x 1/8". The RF grid support rings are strung with nickel wire rather than tungsten mesh in order to maintain as high a transmission as possible through the RF system. The geometric transmission of a single grid strung with nickel wire is approximately 97 per cent.

The 20 stage radio-frequency mass spectrometer had been previously tested independently on a test apparatus in order to insure that the open type structure would function properly. The mass analyzer was found to be operating well and had a maximum resolution of about 30, defined by, resolution = $M_p/(M_2-M_1)$, where M_p is the mass corresponding to the peak and (M_2-M_1) is the mass difference at 10 per cent peak height.

Figure 1 shows the DC retarding experiment collision chamber. The top grid of the reaction region, electrode A,

was kept at ground potential in order to shield the secondary collector, B and F, from changes in the potential of the DC retarding grid, electrode R.

The fast product ions and primary beam were turned back by adjusting the potential on electrode R, V_R, and collected on the reaction region electrode walls, B and F. The path length of the reaction region was taken as the distance from the electrode B to the mid-plane of electrode R. Since a potential difference, V_R, exists between electrodes A and R an uncertainty is introduced to the path length, ℓ, due to the inhomogeniety of the primary beam energy in this region. A discussion of this error is given in a later section.

The primary beam current was monitored throughout the process of making the measurements and was found to be very steady; in fact, no corrections due to drift in total beam current were necessary. The primary beam current was measured with a General Radio Amplifier and Electrometer model 1230-A and recorded on one channel of a Varian Dual Channel Recorder model G-22; this detection system is capable of measuring currents as small a 1×10^{-13} amps. The secondary ion current was measured with a Carey Model 31 Vibrating Reed Electrometer and recorded on a Leeds and Northrup Speedomax recorder; this detection system is capable of measuring currents as small as 1×10^{-15} amps.

The sinusoidal RF voltage was supplied by a Hewlett-Packard Signal Generator model 606A with a frequency span from

50 kc to 65 mc. The RF signal from the signal generator was fed through Hewlett-Packard Wide Band Amplifiers models 460AR and 460BR, in cascade, in order to give an output voltage of about 8 volts rms. The RF voltage was monitored with a Hewlett-Packard Vacuum Tube Voltmeter model 410B.

The apparatus is differentially pumped by high-speed mercury diffusion pumps connected to liquid nitrogen cooling traps. The ion source and collision chamber are separated from their adjacent chambers by defining electrodes with 2 mm holes. The pumping system is capable of maintaining a pressure of approximately 1×10^{-6} mm Hg in the fore, magnet, and post chambers, while the ion source is charged with gas at a backing pressure of about 0.1 mm Hg. The background gas pressure in the collision chamber, was 5×10^{-6} mm Hg or lower. The scattering gas pressures were read with a precision McLeod gauge, and for the cross-section measurements were in the range from 4×10^{-4} to 1×10^{-3} mm Hg. The difference in mercury levels was read with a small cathetometer which was accurate to $\pm$ 0.01 mm.

Measurements

DC retardation experiment

After the beam was focused to optimum intensity and determined to be steady an energy analysis on the primary beam was done. This was done first under empty tube or vacuum conditions by increasing V_R positive with respect to the reaction

region with electrode A at ground potential. The product ion detection system was set at a high sensitivity capable of detecting product ions. V_R was increased slowly; from 0.05 to 5.0 volts in 0.20 volt increments, and from 5.0 volts to the point of total beam retardation in 0.5 volt increments. The current was recorded by the product ion detection system.

This type of empty tube retardation serves three purposes, namely:

(a) to correct for any product ions formed by virtue of collisions of the primary ions with the background gas

(b) to give an energy analysis of the primary beam

(c) to measure and record the total beam current under no gas conditions.

Upon completion of the empty tube retardation scattering gas was admitted into the collision chamber through a Vactronic vari-vac VV-503 leak valve connected to a storage bulb, and the collision chamber pressure was measured with the McLeod gauge. The tank hydrogen used as the source of H_2 scattering gas was further purified by adsorption on degassed charcoal at liquid nitrogen temperatures. The tank argon used was not purified further; it was estimated by the manufacturer to be 99.9 per cent pure. The retardation was then carried out in the same manner as for the empty tube condition. From the resulting product ion current versus V_R obtained for gas-in conditions the empty tube correction must be subtracted point by point in order to determine the amount of product ions

produced by reactions with scattering gas at known density. Figures 5, 6, 7, and 8 are examples of the resulting corrected data. The interpretation and structure of these curves will be discussed in detail in a later section.

A pressure dependence of the inelastic cross-section was determined for both systems studied by measuring the inelastic cross-section at different pressures. It was found that the total inelastic cross-section was constant over a pressure range from 1×10^{-4} to 5×10^{-3} mm Hg. However, the ratio of the current due to charge transfer to the current due to total reaction was not constant at the higher end of this pressure range. This ratio was found to increase with increasing pressure. Hence, the criterion used to determine the pressure independent region was the constancy of this ratio. The pressure independent region was found to be from 5×10^{-4} to 1.2×10^{-3} mm Hg.

It was further found that in the pressure independent region the total ion current (product ions plus unscattered beam) with scattering gas in was the same as the primary beam current under no-gas conditions as measured and recorded by the product ion detection system. That these two currents were the same is probably due to the fact that there was negligible loss due to elastic scattering in the defining chamber because the pressure independent region was low. Because these two currents are the same the total beam current passing electrode D and entering the reaction region is the same under empty tube conditions and gas-in conditions; hence, a normalization of the empty tube correction is not necessary.

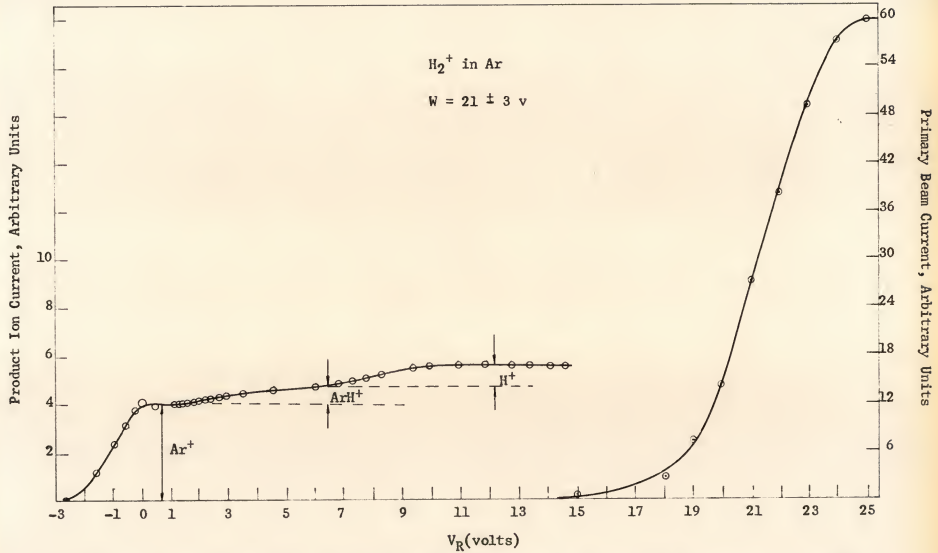

Figure 5.—Retardation Plot for H_2^+, Ar; Showing Extraction and Energy Analysis of Primary Beam

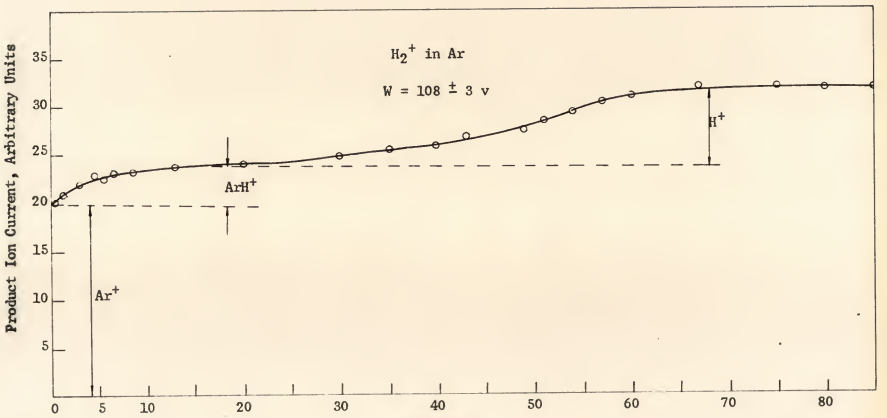

Figure 6.—Retardation Plot for H_2^+, Ar

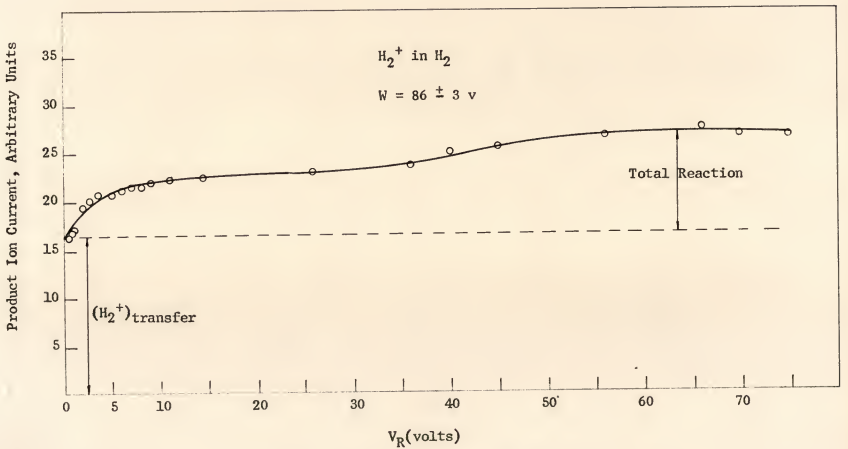

Figure 7.—Retardation Plot for H_2^+ in H_2

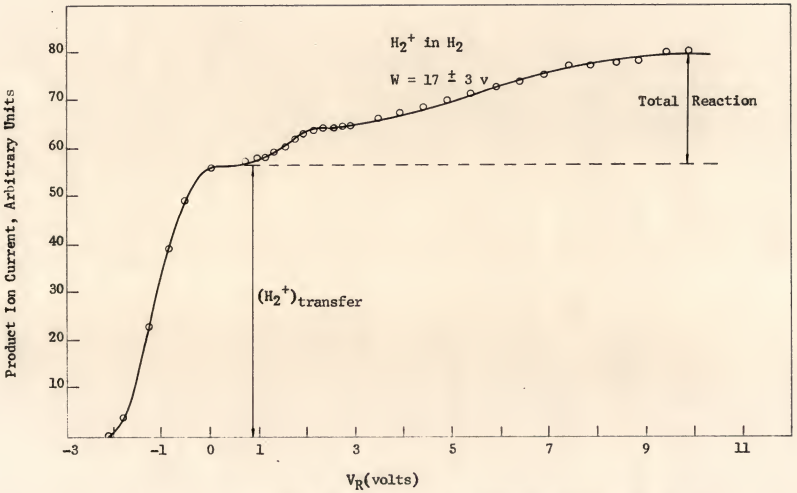

Figure 8.—Retardation Plot for H_2^+ in H_2; Showing Effect of Extraction

RF experiment

In the RF experiment the reaction region must be at some positive potential with respect to ground for the following reasons:

(a) the ions to be mass analyzed, in particular the product ions, must be accelerated before they enter the RF region

(b) the RF region cannot be put off ground because it is inconvenient to have the RF signal generator and amplifiers off ground.

The reaction region was operated at +100 volts so that the energy of the product ions as they entered the RF region was about 100 volts. The target, electrode T, serves to monitor the primary beam.

When the beam was focused to optimum intensity and steady conditions prevailed scattering gas was introduced into the collision chamber. The potential of electrode A, V_A, can be set to extract or retard the slow product ions due to charge transfer. The potential of the RF ion-retarder, V_{IR}, was then set so that no current reaches the secondary collector; then V_{IR} was further increased, usually by about 20 volts, in order to mass analyze. RF voltage was placed on the RF electrodes and the frequency was slowly varied throughout the region of interest.

The peaks due to product ions appear as shown in Figure 9. The structure of these mass spectra will be discussed later. Once the peaks have been identified it is necessary to

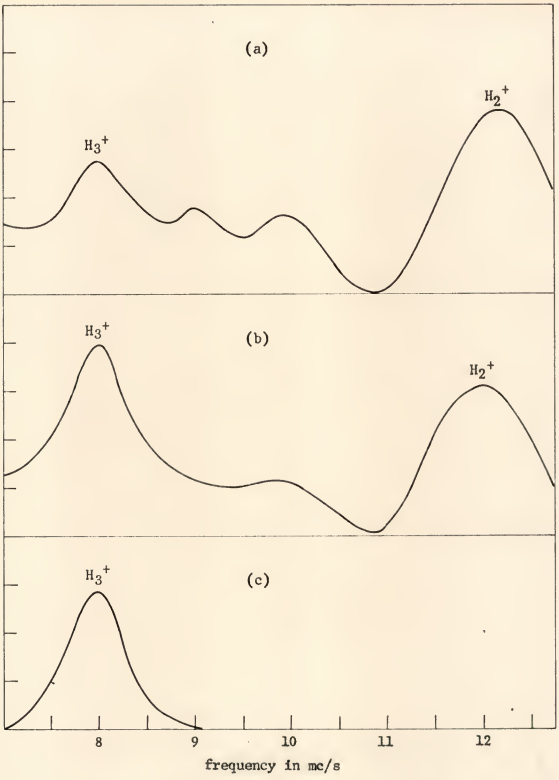

Figure 9.—Radio-Frequency Mass Spectra for H_2^+ in H_2
(a) $V_A = 0.06$, (b) $V_A = 0.08$, (c) $V_A = 1.0$

determine their energy gained through the RF region. This is done by finding the resonant peak of a product ion and increasing V_{IR} until the product ion peak disappears. Other parameters being equal, the resolution is dependent on the ratio $V_{IR}/(\Delta W)_{max}$, that is, the ratio of the potential barrier imposed to the energy gained through the RF region. Since the product of resolution and collection efficiency is a constant it is clear that in order to obtain meaningful relative cross-sections the resolutions for all product ions must be known and equal. The ratio of the peak heights, corrected for target interception, of two product ions examined under the same resolution, will then be proportional to the relative cross-sections of the two processes forming these ions.

CHAPTER III

CALCULATIONS AND RESULTS

An ion beam traversing a path of length ℓ through a gas at a number density N will be attenuated according to the well known expression (Beer's law),

$$I_p = I_T \, e^{-N\sigma_T \ell} \qquad [1]$$

where,

I_p = the unscattered primary current after passing through the reaction region

I_T = the primary current entering the reaction region

ℓ = the path length of the reaction region

σ_T = the total inelastic cross-section for the removal of beam particles by collisions in cm^2

N = number density of target gas molecules in cm^{-3}.

Elastically scattered ions were not detected in this experimental arrangement, so that only inelastic processes contribute to σ_T.

Clearly, $(I_T - I_p) = I_s$, is the total current produced by inelastic collisions. Let us write

$$I_s = (I_T - I_p) = \sum_j I_j \quad , \qquad [2]$$

where I_j represents product ion current due to a particular inelastic process signified by j. Then the cross-section for

a particular process j, σ_j, has the following relationship to the total inelastic cross-section;

$$\sigma_j = \frac{I_j}{\sum_j I_j} \sigma_T \quad . \qquad [3]$$

Substituting [2] and [3] into [1] one obtains the expression for σ_j as

$$\sigma_j = \frac{1}{N\ell P} \cdot \left[\frac{I_j}{I_s}\right] \mathrm{Ln}\left[1 + \frac{I_s}{I_p}\right] \quad . \qquad [4]$$

All the cross-sections reported were obtained from the DC retardation experiment and were calculated using equation [4].

The calculated results are tabulated in Table 1 for the H_2^+, H_2 system. σ_t is the charge transfer cross-section; and σ_r is the total reaction cross-section, exclusive of charge transfer. It is referred to as the total reaction cross-section since it was not possible to distinguish the products of the ion-molecule reaction $H_2^+ + H_2 = H_3^+ + H$ and the dissociation reaction, $H_2^+ + H_2 = H^+ + H + H_2$.

The calculated results for the H_2^+, Ar system are tabulated in Table 2. σ_t is the charge transfer cross-section, σ_i is the ion-molecule reaction cross-section for the process $H_2^+ + Ar = ArH^+ + H$, and σ_d is the collision-induced dissociation cross-section for the process $H_2^+ + Ar = H^+ + H^+ Ar$.

The raw data, measured and recorded by the secondary detection system were the product ion current as a function of V_R, I_p, the primary beam current, and the incident ion energy, W,

TABLE 1

TABULATION OF CROSS-SECTIONS FOR H_2^+, H_2

W(ev)	$\sigma_t \times 10^{16}$ cm^2	$\sigma_r \times 10^{16}$ cm^2
13	13.9	6.7
17	13.8	5.7
20	16.7	5.2
29	14.2	5.7
40	13.6	6.6
50	13.2	5.4
58	12.4	4.8
62	12.4	5.5
75	10.9	7.1
81	9.8	3.6
86	11.6	7.4
98	12.9	6.2
117	8.0	8.6

TABLE 2

TABULATION OF CROSS-SECTIONS FOR H_2^+, Ar

W(ev)	$\sigma_t \times 10^{16}$ cm^2	$\sigma_i \times 10^{16}$ cms	$\sigma_d \times 10^{16}$ cm^2
12	10.8	3.8	3.6
16	14.0	3.3	7.7
20.5	13.7		
27.5	15.1	2.9	6.5
34	15.9	2.7	5.8
43	13.4	2.7	3.5
45	12.7	2.0	5.0
53	14.2	1.8	5.0
58	13.1	2.2	5.3
66	15.5	3.1	4.9
75	15.1	2.9	7.8
83	12.8	4.1	6.7
93	11.7	3.7	6.5
108	16.2	2.8	6.7
135	15.0	4.0	6.7

obtained from an energy analysis. The other data were the path length, ℓ, the pressure of the scattering gas, and the ambient temperature around the collision chamber.

The measurable quantities which are subject to random errors are;

(a) the current ratio $[I_j/I_s]$

(b) the current ratio $[I_s/I_p]$

(c) the path length ℓ

(d) the pressure P.

It is pertinent to estimate the maximum errors associated with each quantity. Since the measurable currents, I_j, I_s, and I_p are not independent of each other the current ratios (a) and (b) have different random errors. For example, for the H_2^+, Ar system I_j can be I_t, the current due to charge transfer, I_i, the current due to ArH^+ from the ion-molecule reaction, or I_j, the current due to H^+ from the collision-induced dissociation reaction and depending upon the size of the different currents and the method of measurement, the ratios I_s/I_p, I_t/I_s, I_i/I_s, and I_d/I_s will have different maximum errors. The estimated maximum error of the measurable current ratios used to calculate the cross-sections for the H_2^+, Ar system are; for I_t/I_s, $\pm$ 3 per cent, for I_i/I_s, $\pm$ 10 per cent, for I_d/I_s, $\pm$ 10 per cent and for I_s/I_p, $\pm$ 2 per cent.

A random error is introduced by the uncertainty of the path length, ℓ. This uncertainty in ℓ is due to the inhomogeniety of the primary beam energy between electrodes A and R

and is not amenable to direct calculation. The inhomogeniety of the primary beam energy is a function of V_R; hence it will affect the product ion currents of the different processes, measured as a function of V_R, in different ways. The charge transfer current is measured with V_R = +0.05 volts, the ion-molecule reaction current is measured with $V_R \approx 0.14(W_p)$, and the collision-induced dissociation reaction current is measured with $V_R \approx 0.60(W_p)$. The distance between electrodes A and R is 25 per cent of the total path length. Furthermore, the affect of this inhomogeniety will be largest if the cross-section changes rapidly with the incident ion energy. Using the calculated cross-section as a first approximation of the functional dependence upon energy, the considerations involving V_R and the measurements of the different currents, and the fact that the distance over which there is uncertainty is 25 per cent of ℓ the estimates of the maximum errors due to this effect are: essentially no error to the charge transfer cross-section, an error of $\pm$ 3 per cent to the ion-molecule reaction cross-section, and an error of $\pm$ 8 per cent to the collision-induced dissociation cross-section. The random error in the pressure measurement is estimated to be $\pm$ 2 per cent. The energy spread of the incident ion beam energy is $\pm$ 3 volts.

Neglecting the logarithmic term in equation [4] and applying the propagation-of-error treatment (14) to equation [4] the estimated relative errors in the cross-sections are;

(a) for σ_t, $\pm$ 5 per cent

(b) for σ_i, $\pm$ 15 per cent

(c) for σ_d, $\pm$ 20 per cent

For the H_2^+, H_2 system the estimated errors are;

(a) for σ_t, $\pm$ 5 per cent

(b) for σ_r, $\pm$ 15 per cent

The estimated error of the measurement of the absolute total inelastic cross-section, $\sigma_T = \sum_j \sigma_j$, for both systems is $\pm$ 10 per cent.

A measure of the reliability of the measurements can be seen by comparing the value of the charge transfer cross-section of H_2^+ in H_2. These cross-sections were determined during a pressure dependence study for this sytem. All three pressures were in the pressure independent region.

Charge Transfer Cross-Section	Pressure, mm Hg	Error Deviation From Average
12.75×10^{-16} cm^2	4.412×10^{-4}	0.083
12.95×10^{-16} cm^2	1.042×10^{-3}	0.117
12.80×10^{-16} cm^2	1.693×10^{-3}	0.033

The errors shown above, taken as the difference between the actual value and the average value of the three measurements, lead to a root mean square error of $\pm$ 0.7 per cent.

CHAPTER IV

DISCUSSION

The H_2^+, Ar System

Charge Transfer

The slow ion current due to charge transfer, I_t, is taken as that current that reaches the reaction region walls, electrodes B and F, with V_R set at +0.05 volts with respect to the reaction region. This product ion current includes the slow ions that are initially traveling at approximately 90° to the beam axis as they leave the immediate collision region plus any slow ions that are not capable of overcoming V_R (+0.05). Hence, it is possible that some current due to ArH^+ is counted as charge transfer since the minimum energy that ArH^+ can have is 0.429 per cent of the incident energy. However, the error introduced in the charge transfer current is probably quite small above 10 ev incident ion energy. The current to B and F was completely extracted from the reaction region when electrode R and A were set at -3.0 volts with respect to the reaction region. Usually half of I_t was extracted with V_R and V_A set at -0.5 volt; which shows that the current I_t was due entirely to slow ions, which had a mean initial energy of about 0.1 to 0.2 ev.

The charge transfer cross-section, σ_t, varies with the relative energy of collision as shown in Figure 10. Three

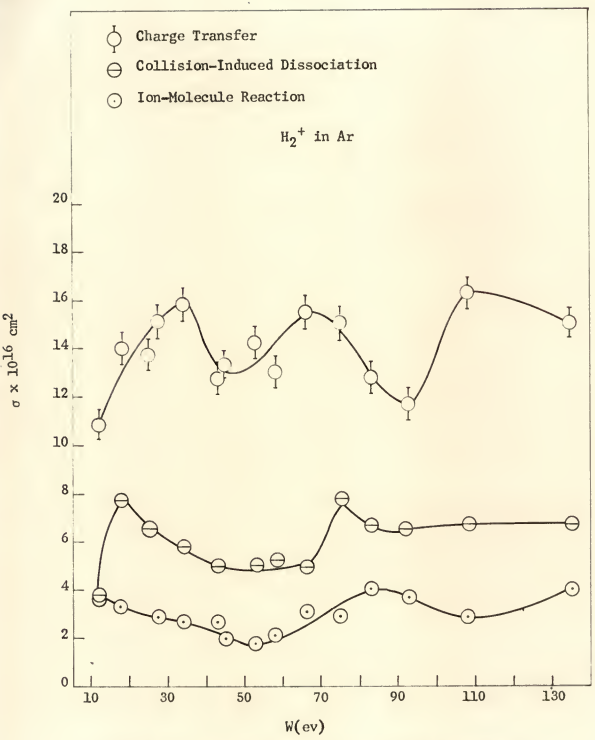

Figure 10.—Cross-Sections vs. Incident Ion Energy, W

broad maxima were found in the energy range studied at ion energies equal to 110 volts, 65 volts, and 34 volts. The lines extending from the experimental points for charge transfer in Figure 10 extend to the estimated maximum error; hence, it can be seen that the variations in the cross-sections are significant. These "fine structure" maxima can best be explained in terms of the excited states of the H_2^+ incident ion with the aid of "Massey's criterion" (15), more commonly referred to as the adiabatic hypothesis.

In brief, the adiabatic hypothesis states that the cross-section for an inelastic process with an energy defect, ΔE, will be small when $[\underline{a}\ |\Delta E|\ /hV] \gg 1$, rise as $[\underline{a}\ |\Delta E|\ /hV]$ approaches 1, and begin to fall off after exhibiting a maximum around $[\underline{a}\ |\Delta E|\ /hV] = 1$. In the above expression $|\Delta E|$ is the absolute value of the energy defect in ev. V is the relative velocity, h is Planck's constant, and $\underline{a}$ is a number the order of atomic dimensions.

J. B. Hasted (16-20) has accumulated a large amount of data in support of the adiabatic hypothesis. Reference (16) is an excellent review article by Hasted and contains an immense number of references to studies of inelastic collisions. Hasted and other workers have found maxima in the charge transfer cross-section for various systems. Hasted found that a best fit through these data, plotted as $|\Delta E|\ \sqrt{M}$ vs. $\sqrt{W}$ yields a value of $\underline{a}$ equal to 8 $\mathring{A}$ (16).

Figure 11 shows a plot of $[\underline{a}\ |\Delta E|\ /\hbar V] = 1$, the adiabatic theory expression for maximum cross-sections. The slope, corresponding to $\underline{a} = 8$ Å, was drawn through the origin in order to determine whether the various maxima observed for the charge transfer cross-section correspond to reasonable values of the energy defect. The ΔE's corresponding to the three maxima for H_2^+, Ar are seen to be 0.5, 0.4, and 0.29 ev. It should be noted that the value of $\underline{a} = 8$ Å was obtained from charge transfer data where most of the systems exhibited maxima in the range from 1 Kev to 1 Mev incident ion energy. The extrapolation of this value down to much lower incident ion energies is doubtful since $\underline{a}$ is probably best described as a function of relative velocity (15). However, even if one allows for a rather wide variation in the value of $\underline{a}$, that is a change in slope in Figure 11, it can be seen that the range of the ΔE's is between 0.1 and 1.0 ev.

The energy defects which are found by making this extrapolation fall in the range of energy defects corresponding to charge transfer if one considers the incident H_2^+ ions are in vibrationally excited states. Marmet and Kerwin (21) have shown that the most probable transition for the formation of H_2^+ from H_2 in the ground state by electron impact is to the third (v=3) vibrationally excited state of the molecular ion, H_2^+. Since H_2^+ was formed in a source using 100 ev electrons it is quite reasonable to assume that the H_2^+ ions are in a distribution over vibrationally excited states which is peaked about v = 3.

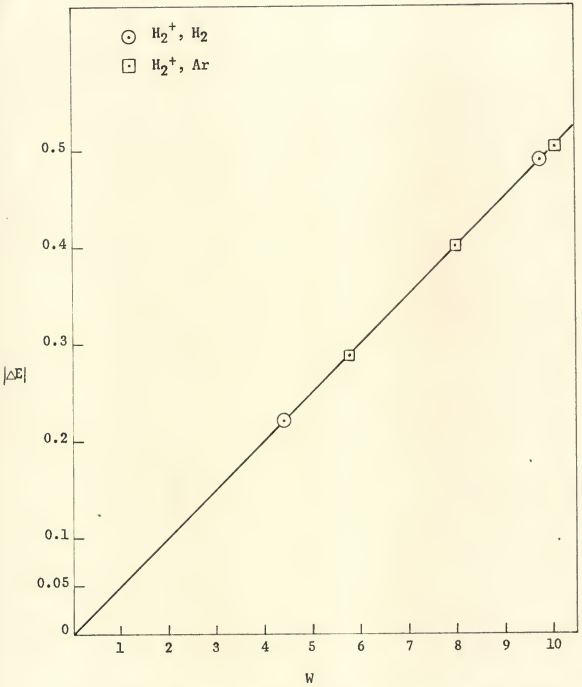

Figure 11.—Plot of Adiabatic Theory Expression [a |ΔE| /hV] = 1, for a = 8 Å

The following charge transfer reactions are some of the many reactions that may be contributing to the observed maxima:

$$H_2^+(v=3) + Ar = Ar^+(g) + H_2(v=2); \quad \Delta E = -0.593 \text{ ev} \qquad [1]$$

$$H_2^+(v=0) + Ar = Ar^+(g) + H_2(v=0); \quad \Delta E = -0.333 \qquad [2]$$

$$H_2^+(v=3) + Ar = Ar^+(g) + H_2(v=1); \quad \Delta E = -0.062 \qquad [3]$$

$$H_2^+(v=3) + Ar = Ar^+(I) + H_2(v=0); \quad \Delta E = +0.250 \qquad [4]$$

$$H_2^+(v=3) + Ar = Ar^+(g) + H_2(v=0); \quad \Delta E = +0.427 \qquad [5]$$

$$H_2^+(v=4) + Ar = Ar^+(g) + H_2(v=0); \quad \Delta E = +0.630 \qquad [6]$$

In the above reactions (g) represents the ground state of Ar^+, $^2P_{3/2}$ (I) represents the first excited state of Ar^+, $^2P_{1/2}$, and $\Delta E > 0$ represents an exoergic process. All of these reactions could be contributing to the observed structure in the variation of the charge transfer cross-section with relative velocity. Hasted and Smith (19) have found a maximum for the H_2^+, Ar system charge transfer at W = 110 volts which they attributed to reaction [2]. Whether this maximum corresponds to reaction [2] is somewhat doubtful due to the difficulty in matching the various possible reactions with the maxima. The two main difficulties in identifying the maxima with specific reactions are; (a) the value of a is uncertain in this energy range and (b) the energy range studied in this work is not broad enough to lead to a conclusive decision. The value of the maximum for charge transfer at W = 110 volts found by Hasted (19) was 7.5×10^{-16} cm^2 to be compared with the present maximum value at W = 110 volts of 16.5×10^{-16} cm^2 found in this work. Since

Hasted obtained only two cross-sections at energies lower than 110 volts a detailed comparison of this work and his in this energy range is not meaningful.

Ion-molecule and collision-induced dissociation cross-sections

All ions, other than the primary ions which surmount the DC retarding potential barrier, V_R, set at +0.05 volt are counted as reaction products. The maximum angle of scattering in the laboratory system of coordinates for ArH^+ is 44°. As mentioned earlier in the text the limiting angle for escape from the reaction region is 46.5°. However, in the experimental arrangement used for the DC retardation experiment (Figure 1) the limiting angle must be taken as the angle between a normal line through the 2 mm hole in electrode D and a line from the center of this hole to the inner radius of electrode R. That this must be so can be seen from the fact that the requirement for ions to be counted as reaction products is that they pass through R for some values of V_R and are turned back by higher values of V_R. That is, for this particular arrangement they must pass through R; not just through A. This limiting angle is 41°.

It appears that since the maximum angle of scattering for ArH^+ is 44° and the limiting angle is 41° that some ArH^+ current may be lost, for example, collected on electrode A. It was mentioned earlier that the primary beam current collected an electrodes B and F after retardation by V_R under no-gas

conditions was equal to the total ion current collected on electrodes B and F after retardation by V_R under gas-in conditions. Therefore, there must be only a negligible loss of ArH^+ current. That there is a negligible loss, if any, of ArH^+ current is not surprising; for the limiting angle has its vertex at the 2 mm hole of electrode D and reaction takes place along the entire path length. That is, reactions taking place along the path length, ℓ, have different limiting angle depending on the distance from electrode R.

ArH^+ product ions scattered by an angle θ can pass through electrode R provided that their energy is greater than $0.05/\cos^2\theta$ volt. These products are then turned back by increasing V_R and collected on B and F. Typical retardation plots are shown in Figures 5 and 6. A retardation plot was done for each value of the ion energy. These plots show that there are two distinct energy groups of fast forward scattered ions. One group has a low energy and the other group has an average energy of approximately 40 per cent of the incident ion energy. In all cases, a fairly flat plateau begins at or very near the maximum energy that ArH^+ ions can carry off. This maximum energy corresponds to ArH^+ ions which are scattered through 0°, and is 13.45 per cent of the total energy. On this basis the lower energy group is identified as ArH^+ and its current is used to calculate an ion-molecule reaction cross-section.

The higher energy group of ions may arise from the following processes:

(i) elastically scattered H_2^+

(ii) H_2^+ or H^+ from the ionization reactions

$$H_2^+ + Ar = H_2^+ + Ar^+ + e; \quad \Delta E = 15.755 \text{ or}$$

$$H_2^+ + Ar = H^+ + H + Ar^+ + e; \quad \Delta E = 18.403$$

(iii) collision-induced dissociation

$$H_2^+ + Ar = Ar + H^+ + H; \quad \Delta E = 2.648$$

However, the following considerations will show that the collision-induced dissociation is the most likely process that contributes to this high energy group of ions.

Figures 5 and 6 show that the retardation curve goes into a broad flat plateau long before V_R approaches the primary beam energy. If the current due to elastically scattered H_2^+ were detectable it would be reasonable to expect a gradual rise in the retardation curve as V_R approaches the primary beam energy. Further, an average value of 40 per cent of the incident ion energy corresponds to an angle of scattering of about 40° from the beam axis. This large a deviation due to elastic scattering is not expected. Thus, it can be concluded that the ions observed to have approximately 40 per cent of the primary beam energy are not elastically scattered ions, and that elastically scattered ions are not detected as products in this experiment but are counted as primary ions.

Considering reactions (ii), which give H^+ or H_2^+ products from ionization, it has been observed that the apparent ionization threshold due to atomic or molecular collisions is several times the true ionization potential of the target atom or molecule (2).

Indeed, the cross-section for ionization is very low at low energies and usually does not begin rising until the Kev range of incident ion energies is reached. Further, ΔE = 16.0 ev would correspond to a maximum at about 1.6 Kev.

Reaction (iii), collision-induced dissociation, seems to be the most reasonable reaction to produce the observed results. This reaction, with an energy defect of 2.648 ev in energetically possible throughout the energy range of the measurements. The fact that the H^+ produced carries off approximately 40 per cent of the primary beam energy on the average seems to imply a preference of orientation for the reaction to occur. For the H^+ to carry off approximately 40 per cent of the energy its direction of travel must not be appreciably different from that of the initial direction of the incident H_2^+ ion. This further implies that the reaction is most likely to occur when the H_2^+ is oriented with its axis normal to its direction of travel within the collision region. The H_2^+ then dissociates upon collision, some energy being imparted to the Ar atom, and the H^+ and H atom are deviated through small angles about the initial line of motion, each carrying off approximately 40 per cent of the energy on the average.

The dissociation cross-section dependence upon energy shows maxima at W = 16 volts and at W = 75 volts and a gradual rise above W = 80 volts is suggested. The maxima may be due to vibrationally excited H_2^+.

The observed ion-molecule reaction cross-sections for $H_2^+ + Ar = ArH^+ + H$ cannot be compared directly with any available data. Giese and Maier (9) have studied the H_2^+, Ar system in a double mass spectrometer experiment but their complete data are yet unpublished.

It does seem pertinent to attempt to compare the variation of the ion-molecule reaction cross-section with incident ion energy found in this work with that found by Stevenson and Schissler (8). They find a $1/E_r^{1/2}$ dependence of the phenomenological cross-section Q, where Q is defined by

$$\frac{i(S^+)}{i(P^+)} = n_2 \ell Q \quad ,$$

$i(S^+)$ is the product ion current, $i(P^+)$ is the primary ion current, n_2 is the density of scattering gas, and ℓ is the path length. E_r is the ion repeller voltage and hence is related to the energy that the primary ions have as they react with the neutral molecules while being accelerated out of the ion source. In their particular experimental arrangement the collision energy of the primary ions is not precisely known and their analysis is concerned with the variation of the ratio of secondary ions to primary ions, $i(S^+)/i(P^+)$, with ion repeller voltage.

The $1/E_r^{1/2}$ dependence found for most systems studied by Stevenson and Schissler as well as Lampe, Field, and Franklin (7) is in agreement with the predictions of a theory of ion-molecule

reactions due to Gioumousis and Stevenson (22). Gioumousis and Stevenson obtain this type of dependence for the ion-molecule reaction cross-section by considering the interaction to be due to the long range potential between ions and molecules, namely, $\phi(r) = -e^2\alpha/r^4$, where e is the charge and α is the polarizability. Their theory employs the properties of the classical orbits given by such a potential and calculated by Langevin (23). The general prediction of this theory is that the ion-molecule reaction cross-section will vary as $E_r^{-2/n}$ if the interaction potential $\phi(r)$ is of the form $\phi(r) = \pm K/r^n$.

The ion-molecule reaction cross-section found in this work does not follow a simple $1/E^{2/n}$ law, in the energy range covered by the measurements. However, the cross-sections obtained for the lowest energies seem to suggest that in this region the reaction may be going into this type of dependence. Due to the uncertainty in the energy of the primary ions in an ion source experiment it is difficult to match the values of the ion repeller voltage with the incident ion energy of this experiment. It is estimated that the lowest energies of this work correspond to collision energies at the highest values of the ion repeller voltage used by Stevenson and Schissler. On this basis, then, it seems that below 20 ev ion energy the ion-molecule reaction cross-section may be in a region where the variation with incident ion energy is in accord with the predictions of the theory. However, above 20 ev ion energy the variation does not follow a simple relationship.

A $1/E^{1/2}$ dependence implies that the long range ion-induced dipole forces are solely responsible for the reaction. It was shown by Eyring, Hirschfelder, and Taylor (24) that the long range forces can account for the formation of activated complexes. The ion-molecule reactions then may proceed by a mechanism involving an activated complex at low energies (below 20 ev in this case). At higher incident ion energies the long range forces leading to the formation of activated complexes may not be important and the reactions may proceed by an entirely different mechanism.

The H_2^+, H_2 System

Charge transfer

The variation of the charge transfer cross-section with incident ion energy for the H_2^+, H_2 system is shown in Figure 12. The values of the cross-sections and functional dependence upon energy are in good agreement with those of Cramer (25) except for the maximum observed in this work at W = 98 volts.

Applying similar arguments as those used for the H_2^+, Ar case one notes that the maxima could be due to the existence of populated vibrationally excited states of the incident H_2^+ molecular ion. For example, some reactions for charge transfer that may be written are:

$$H_2^+(v=2) + H_2(v=0) = H_2(v=2) + H_2^+(v=0); \ \Delta E = -0.50 \text{ ev} \qquad [1]$$

$$H_2^+(v=1) + H_2(v=0) = H_2(v=1) + H_2^+(v=0); \ \Delta E = -0.26 \qquad [2]$$

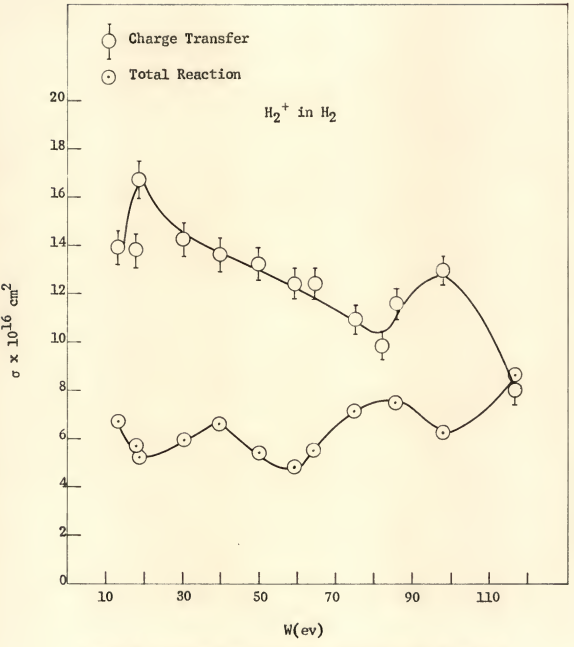

Figure 12.—Cross-Section vs. Incident Ion Energy, W

$H_2^+(v=0) + H_2(v=0) = H_2(v=0) + H_2^+(v=0)$; $\Delta E \simeq 0$ [3]

$H_2^+(v=1) + H_2(v=0) = H_2(v=0) + H_2^+(v=0)$; $\Delta E = 0.27$ [4]

$H_2^+(v=2) + H_2(v=0) = H_2(v=0) + H_2^+(v=0)$; $\Delta E = 0.52$ [5]

$H_2^+(v=3) + H_2(v=0) = H_2(v=0) + H_2^+(v=0)$; $\Delta E = 0.75$ [6]

From Figure 11 it can be seen that the maximum at W = 16 ev corresponds to a $|\Delta E|$ of 0.22 ev and the maximum at W = 98 ev corresponds to a $|\Delta E|$ of 0.49 ev. Clearly, reactions [2], [4], [1], and [5] could be contributing to these observed maxima. Since the target is, in this case, a diatomic molecule there are more vibrational degrees of freedom available than for the H_2^+, Ar system. That is, in the H_2^+, H_2 system both product species may be in vibrationally excited states.

Total reaction cross-sections

Unlike the H_2^+, Ar system ion-molecule reaction products cannot be separated from other reactions that take place on a simple energetic basis. It can be seen from Figures 7 and 8 that no definite plateau exists except for the broad flat plateau that separates the product ions from the primary beam. However, it is to be noted that two groups are suggested even though they are not well separated. This is to be expected since the maximum energy that H_3^+, a likely ion-molecule reaction product, can have is 95 per cent of the initial energy. This maximum energy for H_3^+ corresponds to scattering through 0°. The maximum angle of scattering for H_3^+ is 35.5°, hence all of

the H_3^+ having an energy of at least $0.05/\cos^2\theta$ is capable of surmounting V_R set at 0.05 volt. The fast forward scattered current is then collected on B and F after retardation by V_R and counted as total reaction product current.

The total reaction cross-section dependence upon incident energy appears to exhibit some structure and looks quite similar to the sum of the ion-molecule reaction cross-sections and collision-induced dissociation cross-sections for the H_2^+, Ar system. Since the different reactions contributing to the total reaction cross-sections could not be separated on an energetic basis, any discussion of these cross-sections is necessarily limited. However, it can be concluded that the same type of reactions are suggested on the basis of the similarity of the retardation curves.

The RF experiment

The mass spectra obtained from the H_2^+, H_2 system for W_p = 20 ev are shown in Figure 9 under different potential configurations corresponding to extraction and retardation of product ions due to charge transfer. "Satellite" peaks due to H_2^+ from charge transfer were present under certain conditions of extraction and retardation. These "satellite" peaks were present because it was necessary to mass analyze the product ions under conditions of low resolution since the product ion current was low. Hence, it was imperative to examine the frequency range in question under different conditions of

extraction and retardation in order to tell the difference between "satellite" peaks and product ion peaks. This was accomplished, not without difficulty, by changing the potential conditions and slowly varying the frequency range in question.

The results in Figure 9 show three cases for different potential configurations about the reaction region set by the potential of electrode A, V_A, with respect to the reaction region. They are:

(a) $V_A = 0.06$; this retardation condition is such that the current due to H_2^+ is much larger than the H_3^+ current.

(b) $V_A = 0.08$; this retardation condition is such that the two currents are about equal.

(c) $V_A = 1.0$; this retardation condition is such that the H_2^+ current has been retarded and only the H_3^+ current remains.

V_o, the DC accelerating potential region the ions pass before entering the RF region, was about 80 volts for this experiment. The peak at frequency equal to 12 mc/s corresponds to mass = 2 amu for V_o = 80 volts, the peak at 8 mc/s calculates to mass = 4.5 amu. That this peak at 8 mc/s cannot be due to H_4^+ is easily seen from momentum considerations; in order to conserve momentum any H_4^+ formed in the reaction region must continue to travel in the same direction as the incident H_2^+ ion and hence will strike the target, T. Further, it had been previously observed in various other runs where the conditions of small signal operation were not met that the resonant frequency of an ion was usually lower by about 1 mc/s than that

calculated from the resonant condition equation. In this particular run small signal operation conditions were not met since V_o was only 80 volts. Hence, on the basis of this argument it can be concluded that the peak at 8 mc/s is due to H_3^+.

It was determined that the apparatus was operating well, in as much as the target rid the experiment of the difficulties arising from allowing the primary beam to enter the RF region. Since the target used was large (10 mm in diameter) it intercepted an appreciable fraction of the product H_3^+ current available for mass analysis. This, and the fact that the initial ion current was low, made it impossible to measure an accurate relative cross-section, but this experiment served to identify the H_3^+ product ion. In order to make accurate measurements of relative cross-sections it would be necessary to determine the energy gained through the RF region for each product ion, examine the product ion peaks under the same resolution, and determine a correction for target interception so that the peak heights could be used as a measure of the relative amounts of the species under examination.

The data obtained, however, do lend support to the concept of this experimental arrangement. Further, these data lead to the conclusion that the ion-molecule reaction $H_2^+ + H_2 = H_3^+ + H$ is contributing to the total reaction cross-section measured in the DC experiment.

H^+ product ions were not observed. The similarity in the retardation curves for the two systems studied in the DC

experiment suggests that the collision-induced dissociation reaction cross-section is not small; the absence of H^+ is then significant. The absence of H^+ lends support to the mode of dissociation deduced from the study of the H_2^+, Ar system, that is, that the H^+ and H are deviated through small angles. Since the H^+ is deviated through small angles it is collected on the target and lost to mass analysis.

CHAPTER V

SUMMARY

Two new experiments for the study of ionic collisions have been described. They are: (a) a wide aperature DC retardation experiment and (b) a double mass spectrometer experiment which employs a radio-frequency mass spectrometer for identification of ionic collision products. The combination of the two experiments can lead to accurate results for systems which scatter primarily in the forward direction. The two methods complement each other, in that they give (a) identification of the various possible reactions and (b) cross-sections for these reactions over a range of collision energies.

The DC retardation experiment yields the total inelastic cross-section and in many cases gives a good indication of the energetics of the various reactions that may be taking place by a retardation analysis of the products ions.

The RF experiment employs the same reaction region and DC potential configurations as the DC experiment but includes a wide aperature radio-frequency mass spectrometer and a target to collect and monitor the primary beam after passage through the reaction region. The RF mass analysis region identifies, within limits set by the mass analyzer resolution, the various species formed by collisions. The RF experiment can also give

accurate relative cross-sections for the various possible inelastic processes. In order to determine such relative cross-sections, it is necessary to measure each of the various ion currents at the same mass resolution.

The fact that the reaction region and mass analysis region are open, that is, can accept and mass analyze all products formed that are deviated through less than 46.5°, is a feature that avoids many of the difficulties encountered in an ion source type experiment. Furthermore, product ions emerging from the reaction region in a broad beam do not have to be refocused into a narrow beam in order to enter a mass analysis region, since the RF mass spectrometer is not as sensitive to alignment as other mass spectrometers, e.g., a magnetic deflection type mass spectrometer.

The two systems studied were H_2^+, Ar and H_2^+, H_2 in the energy range from 12 volts to 130 volts incident ion energy. In the H_2^+, Ar system it was possible to separate three inelastic processes;

(a) charge transfer

(b) ion-molecule reaction

(c) collision-induced dissociation

on the basis of the DC retardation experiment alone.

The charge transfer cross-section for H_2^+, Ar shows structure in its variation with incident ion energy. This structure is discussed in terms of the vibrationally excited

state of the incident H_2^+ ions along with the adiabatic hypothesis. It was found that the ion-molecule reaction cross-section, for the most part, does not follow the predictions of an ion-molecule reaction theory due to Gioumousis and Stevenson. The energetics of the collision-induced dissociation reaction imply that there is some preference to orientation for the incident H_2^+. The H_2^+, H_2 system was studied in the DC retardation experiment and in the RF experiment. The energetics of this system were such that it was not possible to separate the ion-molecule reaction cross-section from the total reaction cross-section exclusive of charge transfer. The charge transfer cross-section for H_2^+, H_2 also showed "fine structure." This is discussed in the same terms as that used for the H_2^+, Ar charge transfer. The RF experiment showed that the following ion-molecule reaction, $H_2^+ + H_2 = H_3^+ + H$, was contributing to the total reaction cross-section measured for H_2^+, H_2 in the DC retardation experiment. The H_3^+ peak was separated from the H_2^+ due to charge transfer. It was not possible to determine relative cross-sections with the RF experiment because of insufficient initial ion current. An H^+ product ion peak was not observed, or expected, in this experiment.

LIST OF REFERENCES

1. E. H. Kennard, Kinetic Theory of Gases (McGraw-Hill Book Company, 1938), Chapter III.

2. H. S. W. Massey and E. H. S. Burhop, Electronic and Ionic Impact Phenomena (Oxford University Press, 1952).

3. I. Amdur, J. E. Jordan, S. O. Colgate, J. Chem. Phys. 34, 1952 (1961).

4. W. H. Cramer, J. Chem. Phys. 30, 641 (1959).

5. T. L. Bailey, C. J. May, E. E. Muschlitz, Jr., J. Chem. Phys. 26, 1446 (1957).

6. F. W. Lampe, J. L. Franklin, and F. H. Field, Progress in Reaction Kinetics, Volume 1 (Permagon Press, 1961).

7. F. H. Field, J. L. Franklin, and F. W. Lampe, J. Am. Chem. Soc. 79, 2419 (1957).

8. D. P. Stevenson and D. O. Schissler, J. Chem. Phys. 29, 282 (1958).

9. C. F. Giese and W. B. Maier, J. Chem. Phys. 35, 1913 (1961).

10. L. I. Schiff, Quantum Mechanics, 2nd edition (McGraw-Hill Book Company, 1955).

11. W. H. Bennett, J. Applied Phys. 21, 143 (1950).

12. P. A. Redhead and C. R. Crowell, J. Applied Phys. 24, 331 (1953).

13. W. H. Cramer and J. H. Simons, J. Chem. Phys. 26, 1272 (1957).

14. H. Margenau and G. M. Murphy, The Mathematics of Physics and Chemistry (D. Van Nostrand Company, 1943), p. 498.

15. H. S. W. Massey, Rep. Prog. Phys. 12, 248 (1948-49).

16. J. B. Hasted, Advances in Electronics and Electron Physics, edited by L. Marton (Academic Press, 1960), p. 1.

17. H. B. Gilbody and J. B. Hasted, Proc. Roy. Soc. A238, 334 (1956-57).

18. J. B. Hasted, Proc. Roy. Soc. A205, 421 (1951).

19. J. B. Hasted and R. A. Smith, Proc. Roy. Soc. A235, 354 (1956).

20. J. B. Hasted and J. B. H. Stedeford, Proc. Roy. Soc. A227 466 (1955).

21. P. Marmet and L. Kerwin, Canad. J. of Phys. 38, 972 (1960).

22. G. Gioumousis and D. P. Stevenson, J. Chem. Phys. 29, 294 (1958).

23. P. Langevin, Ann. Chim. Phys. 5, 245 (1905).

24. H. Eyring, J. O. Hirschfelder, and H. Taylor, J. Chem. Phys. 4, 479 (1936).

25. W. H. Cramer, J. Chem. Phys. 35, 836 (1961).

BIOGRAPHICAL SKETCH

Manuel G. Menendez was born on June 15, 1935, in New York City, New York. He attended elementary school in New York and secondary schools in Tampa, Florida. In June, 1958, he received the Bachelor of Chemical Engineering degree from the University of Florida. In September, 1958, he entered the Graduate School of the University of Florida. Since that time he has held a graduate teaching assistantship in the Department of Chemistry, research assistantships in the Department of Electrical Engineering, and held for two years a National Defense Education Act IV Graduate Fellowship in Chemical Physics.

Manuel G. Menendez is married to the former Sandra K. Guerra.

This dissertation was prepared under the direction of the chairmen of the candidate's supervisory committee and has been approved by all members of the committee. It was submitted to the Dean of the College of Arts and Sciences and to the Graduate Council and was approved as partial fulfillment of the requirements for the degree of Doctor of Philosophy.

April 20, 1963

A. H. Goff

Dean, College of Arts and Sciences

Dean, Graduate School

SUPERVISORY COMMITTEE:

E. E. Muschlitz, Jr.

Chairman

T. L. Bailey

Co-Chairman

H. H. Fisher by R. J. Dresden

T. A. Scott

R. J. Hanrahan